中国物理学会
Chinese Physical Society

PAPER

Hybridization Effects Revealed by Angle-Resolved Photoemission Spectroscopy in Heavy-Fermion Ce$_2$IrIn$_8$ [*]

View the article online for updates and enhancements.

Hybridization Effects Revealed by Angle-Resolved Photoemission Spectroscopy in Heavy-Fermion Ce₂IrIn₈ *

Haijiang Liu(刘海江)[1,2], Yuanji Xu(徐远骥)[1,2], Yigui Zhong(钟益桂)[1,2], Jianyu Guan(关剑宇)[1,2], Lingyuan Kong(孔令元)[1,2], Junzhang Ma(马均章)[3], Yaobo Huang(黄耀波)[4], Qiuyun Chen(陈秋云)[5], Genfu Chen(陈根富)[1,2], Ming Shi(史明)[3], Yi-feng Yang(杨义峰)[1,2,6], Hong Ding(丁洪)[1,2,6**]

[1]*Beijing National Laboratory for Condensed Matter Physics and Institute of Physics, Chinese Academy of Sciences, Beijing 100190*
[2]*School of Physics, University of Chinese Academy of Sciences, Beijing 100190*
[3]*Swiss Light Source, Paul Scherrer Institute, CH-5232 Villigen PSI, Switzerland*
[4]*Shanghai Synchrotron Radiation Facility, Shanghai Institute of Applied Physics, Chinese Academy of Sciences, Shanghai 201204*
[5]*Science and Technology on Surface Physics and Chemistry Laboratory, Mianyang 621908*
[6]*Songshan Lake Materials Laboratory, Dongguan 523808*

We utilize high-resolution resonant angle-resolved photoemission spectroscopy (ARPES) to study the band structure and hybridization effect of the heavy-fermion compound Ce₂IrIn₈. We observe a nearly flat band at the binding energy of $7\,\mathrm{meV}$ below the coherent temperature $T_{\mathrm{coh}} \sim 40\,\mathrm{K}$, which characterizes the electrical resistance maximum and indicates the onset temperature of hybridization. However, the Fermi vector and the Fermi surface volume have little change around T_{coh}, which challenges the widely believed evolution from a high-temperature small Fermi surface to a low-temperature large Fermi surface. Our experimental results of the band structure fit well with the density functional theory plus dynamic mean-field theory calculations.

Heavy-fermion compounds, which were first discovered in CeAl₃ in 1975,[1] are among some of the most exotic materials in condensed matter physics. The name originates from the largely enhanced effective mass of the heavy quasiparticles, which can be 2 or 3 orders of magnitude higher than that in a normal metal.[2] These compounds usually contain some Ce, Sm, Yb, U, Pr, Pu, Np elements, which possess an unfilled $4f$ or $5f$ shell. It is widely believed that $4f/5f$ electrons behave as local moments at high temperatures and become itinerant after hybridized with the conduction electrons at low temperatures. Many phenomena have been discovered in heavy-fermion compounds, including antiferromagnetism,[3] ferromagnetism,[4] superconductivity,[5] quantum critical point,[6] quadrupole order,[7] hidden order,[8,9] topological property.[10] Central to understanding these exotic phenomena is the interplay of itinerancy and localization. However, the low energy scales (critical temperature, hybridization gap and superconducting gap) in heavy-fermion systems have brought major challenges to many experimental techniques.

The $\mathrm{Ce}_m T_n \mathrm{In}_{3m+2n}$ ($m = 1, 2, n = 1, 2$ and T: Co, Rh, Ir, Pd, Pt) family is a good platform of heavy-fermion materials for studying the interplay between c–f hybridization, magnetism, superconductivity, quantum criticality, and so on. $\mathrm{Ce}_m T_n \mathrm{In}_{3m+2n}$ crystallizes with a tetragonal unit cell that can be viewed as m-layers of CeIn₃ unit stacked sequen-

tially with intervening n-layers of TIn₂ along the c-axis. Among them, the spin-glass state observed in Ce₂IrIn₈ indicates partially delocalized Ce $4f$ electrons.[11] The magnetism in Ce₂IrIn₈ depends on Ce-Ir hybridization and local Ce environment. The small but finite onset temperature for spin freezing rules out the quantum critical point (QCP) scenario in Ce₂IrIn₈.[11] High Sommerfeld coefficient ($\gamma \sim 700\,\mathrm{mJ/mol \cdot K^2}$)[12] and the absence of long-range magnetic order indicate an itinerant behavior of Ce $4f$ electron. The μSR Knight-shift experiments[13,14] observed a 'Knight-shift anomaly', in which the Knight shift constant K no longer scales linearly with the susceptibility below a characteristic temperature T_{coh}, which is in agreement with the 'two-fluid' model of heavy-fermion formation.[15] Resistivity measurements showed a broad maximum near 40–$50\,\mathrm{K}$,[13,16] manifesting the development of a coherent state. Angle-resolved photoemission spectroscopy (ARPES) is a powerful tool to directly measure the electronic structure and Fermi surface of solid state materials. Especially, resonant ARPES with photon energies near $120\,\mathrm{eV}$ has been proved to be effective in tracing subtle changes of the $4f$ electrons in the Ce-based heavy-fermion compounds.[17−21] However, systematic temperature-dependent ARPES results on the electronic structure of Ce₂IrIn₈ are still lacking to reveal the hybridization process.

In this Letter, we perform a systematic electronic

structure study on Ce_2IrIn_8 using ARPES measurements and DFT+DMFT calculations to investigate the localized/itinerant nature of the f electrons in its ground state. We find a nearly flat band at the Γ point at low temperatures. Bands away from the Γ point have no flat character, indicating the Ce $4f$-electron contribution appears mainly around the Γ point, which is similar to other cerium based heavy-fermion compounds.[17−19] We also find that Ce_2IrIn_8 has a similar band structure with the $CeMIn_5$ (M=Co, Rh, Ir) compounds near the Fermi level: hole pockets around the Γ point and electron pockets around the M point. Neither in our experimental nor in theoretical explorations could we find large change of the Fermi surfaces at very low temperature, which is different from the widely believed evolution from small Fermi surfaces at high temperatures to large Fermi surfaces at low temperatures.

High-quality single crystals of Ce_2IrIn_8 were grown by flux method. Electrical resistivity was measured with the four-probe method. ARPES data in Fig. 1 were obtained at the SIS beamline of Swiss Light Source using a SCIENTA R4000 analyzer. Samples were cleaved *in situ* along the (001) plane at $T = 15\,K$, and the vacuum was kept below 5×10^{-11} mbar. Other ARPES data were obtained at the 'Dreamline' beamline of Shanghai Synchrotron Radiation Facility (SSRF). Samples were cleaved *in situ* at $T = 10\,K$, and the vacuum was kept below 1×10^{-10} mbar. The overall energy resolution was better than 18 meV.
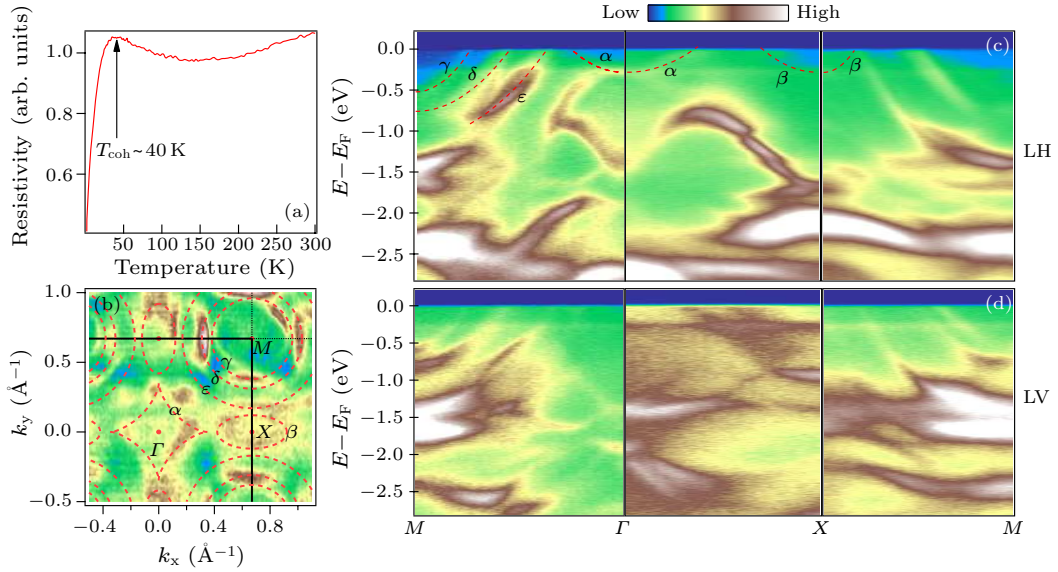
Fig. 1. Electrical resistivity, Fermi surface and polarization dependent band structure along the high symmetry axes. (a) Electrical resistivity of Ce_2IrIn_8. (b) ARPES intensity plot integrated over a window of ($E_F − 10\,meV$, $E_F + 10\,meV$) with circular polarization photons, representing Fermi surfaces of Ce_2IrIn_8. (c) Band dispersions along M–Γ–X–M momentum path with LH polarization. The red-dashed pockets in (b) and the red-dashed lines in (c) indicate the Fermi pockets and corresponding band dispersions, respectively. (d) The same as (c) but with LV polarization. All the ARPES data were obtained with an off-resonant photon energy $h\nu = 115\,eV$, at $T = 16\,K$.

For the first-principles calculations, we used the DFT+DMFT method[22−24] with the continuous time quantum Monte Carlo (CTQMC)[25] and one-crossing approximation (OCA)[26] as the impurity solver. The lattice was represented using the full potential linear augmented plane wave method with spin-orbit coupling as implemented in the WIEN2k package.[27] We chose the Perdew–Burke–Ernzehof generalized gradient approximation (PBE-GGA) for the exchange-correlation potential.[28] The Coulomb interaction was set to $U = 6.0\,eV$ to obtain the correct coherence temperature. We obtained the self-energy, the density of states and the spectral function in real frequency with analytical continuation in the CTQMC calculations, which were then compared with the OCA results for consistency.

The electrical resistivity of Ce_2IrIn_8 shown in Fig. 1(a) has a broad maximum at $T \sim 40\,K$, which is the coherent temperature of Ce_2IrIn_8. To investigate the basic electronic properties of Ce_2IrIn_8, we measured the Fermi surface and band structure of

Ce_2IrIn_8 at $T = 16\,K$. All the ARPES data in Fig. 1 were obtained with an off-resonant photon energy of 115 eV, which has a small cross section for Ce $4f$ electron and can reveal the non-$4f$ band more clearly. The Fermi surface in the Γ–X–M plane, shown in Fig. 1(b), is composed of five electron pockets. Around the Γ point, there is an electron pocket α with the four-corner star-like shape. The bottom of this electron pocket α is around 0.29 eV below the Fermi level, which is consistent with the Ce $4f_{7/2}$ final state.[29,30] Around the M point, there are three electron pockets γ, δ, ε, with their bottoms around 0.51 eV, 0.76 eV, 1.4 eV below the Fermi level with radii of 0.29 $^{-1}$, 0.36 $^{-1}$, 0.5 $^{-1}$, respectively. Around the X point, there is an elongated electron pocket β with its long axis along the Γ–X direction. Because the slit of the analyzer in the SIS beamline is parallel to the ground, the linear horizon (LH) polarization can be used to detect even parity orbitals and z components, while the linear vertical (LV) polarization is used for detecting pure odd parity orbitals. Comparing Figs. 1(c) and

1(d), the electron pocket α near the $\varGamma$ point is more obvious with LH polarization along both $\varGamma$–X and $\varGamma$–M directions, implying that the electron pocket α should not be d_{xy} or $d_{x^2-y^2}$ orbital. Due to the d_{xz} and d_{yz} orbitals are purely even/odd with respect to the ac mirror plane, and we cannot detect the elec-

tron pocket with LV polarization, indicating that the electron pocket α near the $\varGamma$ point should be the $d_{z^2}^2$ orbital. For other bands near the Fermi level, although there is intensity difference, they can be detected by both LH and LV polarizations, which indicates they are not pure orbitals.
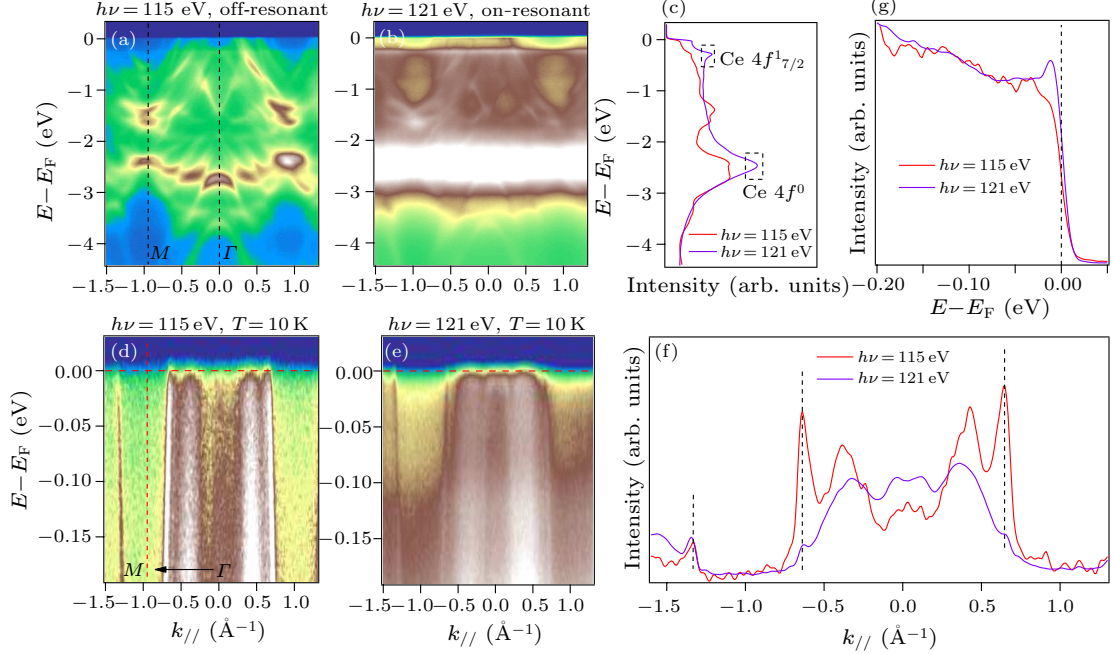
Fig. 2. On/off-resonant ARPES data of Ce$_2$IrIn$_8$ at low temperatures. (a) Off-resonant ($h\nu = 115\,\text{eV}$) intensity plot along the $\varGamma$–M direction at $T = 15\,\text{K}$. (b) The same as (a) but with the on-resonant ($h\nu = 121\,\text{eV}$) photon energy. (c) The angle-integrated EDCs of (a) and (b). (d) Off-resonant intensity plot taken along the $\varGamma$–M direction with $h\nu = 115\,\text{eV}$, $T = 10\,\text{K}$. The vertical dashed red line indicates the position of M. (e) On-resonant intensity plot with $h\nu = 121\,\text{eV}$, $T = 10\,\text{K}$. (f) On/off resonant MDCs at the Fermi level. (g) On/off resonant EDCs at the $\varGamma$ point.

Resonant ARPES measurements were performed at Ce $4d$–$4f$ transition[30] to enhance the Ce $4f$ cross section in Ce$_2$IrIn$_8$. We choose $h\nu = 121\,\text{eV}$ as the resonant photon energy, and $h\nu = 115\,\text{eV}$ as the off-resonant photon energy to minimize the cross section and k_z difference between on/off-resonant photon energy. Figures 2(a) and 2(b) show a photoemission intensity plot taken with off-resonant ($h\nu = 115\,\text{eV}$) and on-resonant ($h\nu = 121\,\text{eV}$) photons at $T = 15\,\text{K}$ along the $\varGamma$–M direction with a circular polarization, respectively. Compared with the on-resonant spectra, the conduction bands dominate the off-resonant spectra. The Ce $4f$ component is strongly enhanced in the on-resonant data, as also shown in the angle-integrated energy distribution curves (EDCs) in Fig. 2(c). Two nearly flat features residing in $0.3\,\text{eV}$ and $2.5\,\text{eV}$ below the Fermi level can be observed in the on-resonant data. Two peaks highlighted in Fig. 2(c) correspond to the Ce $4f_{7/2}^1$ and Ce $4f^0$ final states.[30−32]

Furthermore, fine features near the Fermi level are shown in Figs. 2(d) and 2(e) with a smaller energy window. Figure 2(g) shows the EDCs of Figs. 2(d) and 2(e) at the $\varGamma$ point. Compared with Fig. 2(d), we observed an obvious spectral weight enhancement in the on-resonant data around the $\varGamma$ point near the Fermi level in Fig. 2(e). This enhanced intensity at

the $\varGamma$ point near the Fermi level is actually the tail of Kondo resonance.[33] From the on/off-resonant comparison, we can find that resonant ARPES not only enhances the Ce $4f$ cross section due to the $4d$–$4f$ transition, but also enhances the background making the other bands fuzzy.

To investigate the Fermi vector (k_F) difference due to the f-electron contribution in resonant spectrum, momentum distribution curves (MDCs) at E_F are displayed in Fig. 2(f). We draw three vertical dashed lines to mark the k_F positions away from the $\varGamma$ point in Fig. 2(f). As shown in Fig. 2(f), the on/off resonant MDCs have no visible difference at these marked k_F positions, which indicates the quasi two-dimensional Fermi surfaces centered at the M point, coincide with the results from band calculations of Ce$_2$PtIn$_8$, which has the same crystal structure as Ce$_2$IrIn$_8$.[34] However, on-resonant ARPES suppresses the intensity at $k_F = \pm 0.65^{-1}$, but does not change the k_F value, suggesting that there is no $4f$ contribution involved in this electron pocket centered at the M point, or the hybridization happens far above the Fermi level. The only intensity enhancement in the resonant MDC at the Fermi level is around the $\varGamma$ point. There is an emerging intensity near the $\varGamma$ point compared with the off-resonant ($h\nu = 115\,\text{eV}$) MDC, which indicates that the Ce $4f$ feature near E_F mainly concentrates

around the Γ point. Furthermore, k_F shrinks in the resonant MDC, which also indicates that the f ingre-

dient appears mostly near the Γ point.
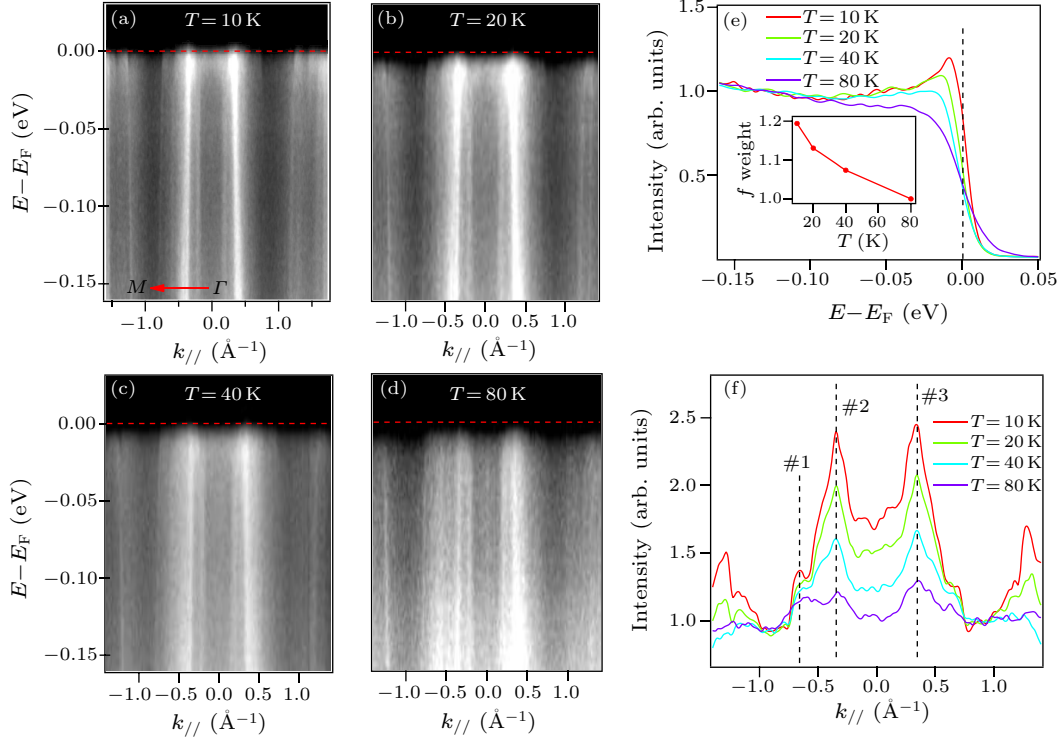
Fig. 3. Temperature-dependent evolution of band dispersion along the Γ–M direction. Intensity plots taken with $h\nu = 121\,\text{eV}$ at (a) $T = 10\,\text{K}$, (b) $T = 20\,\text{K}$, (c) $T = 40\,\text{K}$, (d) $T = 80\,\text{K}$. (e) EDC curves taken at the Γ point at different temperatures. Inset: f-electron weight derived from EDCs with integrated window ($E_F - 100\,\text{meV}$, $E_F + 10\,\text{meV}$). (f) MDCs taken at the Fermi level at different temperatures. The vertical-dashed lines mark the k_F positions.

To trace the hybridization process in Ce$_2$IrIn$_8$, we performed a temperature dependent experiment with the on-resonant photon energy ($h\nu = 121\,\text{eV}$) along the Γ–M direction. At the lowest temperature ($T = 10\,\text{K}$), we observed a nearly flat band near the Γ point at the binding energy about 7 meV. The intensity of this flat band gradually decreases with increasing temperature and nearly disappears above the coherent temperature $T_{\text{coh}} = 40\,\text{K}$. The EDCs show distinct change from a low-temperature peak near the Fermi level to a high-temperature Fermi–Dirac cutoff line shape near the Fermi level in Fig. 3(e), which indicates that the hybridization process happens at low temperatures. Integrating EDCs over the energy range of ($E_F - 100\,\text{meV}$, $E_F + 10\,\text{meV}$), we obtain the T-dependent f-electron spectral weight, as shown in the inset of Fig. 3(e), which displays an obvious increase upon lowering temperature. From our data, we obtain the similar enhancement value ($\sim 20\%$) as the weakly hybridized heavy-fermion compounds CeRhIn$_5$ and CeCoIn$_5$.[18] Furthermore, temperature-dependent MDCs at the Fermi level can in principle reflect the change of k_F around the coherent temperature. However, three vertical-dashed lines in Fig. 3(f) line up the MDC peaks at different temperatures nicely, indicating very small difference in k_F when temperature changes across T_{coh}, which is quite unexpected and contradicts with the small-to-large Fermi surface change scenario expected in these heavy-fermion compounds. However, as we will dis-

cuss in the following, this may occur if there exist several unconnected Fermi surfaces. Similar to our result, there is also no obvious change[18] in k_F in CeRhIn$_5$, even there is a flat band with a sharp peak near E_F.

To understand these results, we carried out DFT+DMFT calculations with experimental lattice parameters for Ce$_2$IrIn$_8$. We carried out strongly correlated calculations using both OCA and CTQMC impurity solvers and found no qualitative difference between the results. We therefore only present the OCA data in the following. Figures 4(a) and 4(b) plot the temperature evolution of the Ce-4f density of states. We can see a sharp quasiparticle resonance developing near the Fermi energy at $T = 10\,\text{K}$ and a rapid increase of the quasiparticle peak when lowering the temperature. The onset temperature of the increase corresponds to the maximum of the temperature derivative of the imaginary part of the self-energy. For $U = 6\,\text{eV}$, this occurs at about 30 K, in a rough agreement with the coherence temperature estimated from experiment, which justifies our choice of parameters. The band structure at 10 K is plotted in Fig. 4(e), exhibiting evident hybridization features near the Fermi energy, which are absent at 200 K. Several features in the corresponding Fermi surfaces are consistent with experiment. Along the X–M direction are four electron bands, two of which are close and difficult to distinguish in ARPES. The bottoms of these bands locate at 0.8 eV and 1.4 eV at the M point, respectively, in good agreement with ex-

periment. These bands show negligible f-character and hence remain unchanged at all temperatures. By contrast, the major f-electron bands at $10\,\mathrm{K}$ locate around the Γ point and along the Γ–X direction, forming a complicated pattern of Fermi surfaces shown in Figs. 4(d) and 4(f), which evolves with lowering temperature due to the local-to-itinerant transition. For example, around the Γ point there exists an electronic pocket, which increases slightly with lowering temperature. This difference agrees with the experimental observation. We also note that the overall change is small compared with the usual expectation of small-to-large Fermi surface change. However, this should not be surprised, if one notices the existence of several electron and hole Fermi surfaces, while each of them varies slightly, a sum of them all would yield the required volume change by the Luttinger theorem. In our ARPES data at $h\nu = 121\,\mathrm{eV}$, each momentum pixel is $0.0095\,^{-1}$, if we assume each of the three electron pockets γ, δ, ε, centered at the M point expands two momentum pixels, we estimate the total Fermi volume expansion to be about 0.078 electrons in the localized-to-itinerant transition. If we add the contributions from the α, β electron pockets, we may obtain similar value 0.2 ± 0.05 in CeCoIn$_5$.[17] More elaborate studies are needed to clarify the exact volume change of these Fermi surfaces.

heavy-fermion compound Ce$_2$IrIn$_8$ across the coherent temperature. We find a nearly flat band near the Fermi level around the Γ point showing no large difference in k_{F}, which seems to challenge the small-to-large Fermi surface scenario in the heavy-fermion compounds. In our case, f-electron orbitals mainly exist near the Γ point but without large changes for k_{F} values and Fermi surface volume. This may be due to multiple Fermi surfaces in this compound. Each single Fermi surface volume varies slightly with temperature and the total effect of multiple Fermi surfaces yields a moderate volume change contributed from Ce $4f$ electrons.

References

[1] Andres K, Graebner J E and Ott H R 1975 *Phys. Rev. Lett.* **35** 1779
[2] Stewart G R 1984 *Rev. Mod. Phys.* **56** 755
[3] Kratochvílová M et al 2015 *Sci. Rep.* **5** 15904
[4] Huy N T et al 2007 *Phys. Rev. Lett.* **99** 067006
[5] Steglich F et al 1984 *Physica B+C* **126** 82
[6] Mito T et al 2003 *Phys. Rev. Lett.* **90** 077004
[7] Tsujimoto M et al 2014 *Phys. Rev. Lett.* **113** 267001
[8] Okazaki R et al 2011 *Science* **331** 439
[9] Mydosh J A and Oppeneer P M 2014 *Philos. Mag.* **94** 3642
[10] Xu N et al 2014 *Phys. Rev. B* **90** 085148
[11] Morris G D et al 2004 *Phys. Rev. B* **69** 214415
[12] Thompson J D et al 2001 *J. Magn. Magn. Mater.* **226** 5
[13] Heffner R H et al 2006 *Physica B* **374** 184
[14] Ohishi K et al 2009 *Phys. Rev. B* **80** 125104
[15] Yang Y and Pines D 2008 *Phys. Rev. Lett.* **100** 096404
[16] Sakamoto I, Shomi Y and Ohara S 2003 *Physica B* **329** 607
[17] Chen Q Y et al 2017 *Phys. Rev. B* **96** 045107
[18] Chen Q Y et al 2018 *Phys. Rev. Lett.* **120** 066403
[19] Chen Q Y et al 2018 *Phys. Rev. B* **97** 075149
[20] Im H J et al 2008 *Phys. Rev. Lett.* **100** 176402
[21] Souma S et al 2008 *Physica B* **403** 752
[22] Kotliar G et al 2006 *Rev. Mod. Phys.* **78** 865
[23] Haule K, Yee C H and Kim K 2010 *Phys. Rev. B* **81** 195107
[24] Held K et al 2008 *J. Phys.: Condens. Matter* **20** 064202
[25] Werner P et al 2006 *Phys. Rev. Lett.* **97** 076405
[26] Pruschke T and Grewe N 1989 *Z. Phys. B* **74** 439
[27] Blaha P, Schwarz K, Madsen G K H, Kvasnicka D and Luitz J 2001 *WIEN2K: An Augmented Plane Wave Plus Local Orbitals Program for Calculating Crystal Properties* edited by Schwarz K (Austria: Vienna University of Technology)
[28] Perdew J P, Burke K and Ernzerhof M 1996 *Phys. Rev. Lett.* **77** 3865
[29] Ito T et al 2003 *J. Phys.: Condens. Matter* **15** S2149
[30] Sekiyama A et al 2000 *Nature* **403** 396
[31] Fujimori S et al 2006 *Phys. Rev. B* **73** 224517
[32] Raj S et al 2005 *Phys. Rev. B* **71** 224516
[33] Patil S et al 2016 *Nat. Commun.* **7** 11029
[34] Klotz J et al 2018 *Phys. Rev. B* **97** 165120

Fig. 4. DFT+DMFT calculations for Ce$_2$IrIn$_8$. (a) Comparison of the density of states of Ce-$4f$ electrons at high temperature ($T = 200\,\mathrm{K}$) and low temperature ($T = 1\,\mathrm{K}$). (b) Temperature evolution of the quasiparticle peak, the imaginary part of the Ce-$4f$ self-energy for $J = 5/2$ manifold at the Fermi energy and its temperature derivative. The solid lines are guide for the eyes fitted using the log-normal and Hill equation functions. [(c), (e)] The momentum-resolved spectral functions at $T = 200\,\mathrm{K}$ and $T = 10\,\mathrm{K}$, respectively. [(d), (f)] The corresponding Fermi surfaces at $T = 200\,\mathrm{K}$ and $T = 10\,\mathrm{K}$.

In summary, we have performed high-resolution on-resonant temperature-dependent study on the